Inorg. Chem. **2008**, *47*, 8798−8806

Inorganic Chemistry
Article

Phenyltin-Substituted 9-Tungstogermanate and Comparison with Its Tungstosilicate Analogue

Santiago Reinoso,[†] Michael H. Dickman, Antonia Praetorius, Luis Fernando Piedra-Garza, and Ulrich Kortz*

School of Engineering and Science, Jacobs University, P. O. Box 750 561, 28725 Bremen, Germany

Received May 9, 2008

Reaction of $(C_6H_5)SnCl_3$ with $Na_{10}[A\text{-}\alpha\text{-}GeW_9O_{34}]$ in water results in the monomeric, trisubstituted Keggin species $[\{(C_6H_5)Sn(OH)\}_3(A\text{-}\alpha\text{-}GeW_9O_{34})]^{4-}$ (**1**), constituting the first organotin derivative of a trilacunary Keggin tungstogermanate. Polyanion **1** could be obtained as two different cesium salts depending on the applied isolation strategy: $Cs_3Na[\{(C_6H_5)Sn(OH)\}_3(A\text{-}\alpha\text{-}GeW_9O_{34})]\cdot 9H_2O$ (**CsNa-1**) and $Cs_3[\{(C_6H_5)Sn(OH)\}_3(A\text{-}\alpha\text{-}HGeW_9O_{34})]\cdot 8H_2O$ (**Cs-H1**). The monomeric phenyltin-containing tungstosilicate $[\{(C_6H_5)Sn(OH)\}_3(A\text{-}\alpha\text{-}SiW_9O_{34})]^{4-}$ (**2**) and the dimeric, sandwich-type derivative $[\{(C_6H_5)Sn(OH)\}_3(A\text{-}\alpha\text{-}H_3SiW_9O_{34})_2]^{8-}$ (**3**) have also been isolated as the cesium salts $Cs_3Na[\{(C_6H_5)Sn(OH)\}_3(A\text{-}\alpha\text{-}SiW_9O_{34})]\cdot 9H_2O$ (**CsNa-2**), $Cs_4[\{(C_6H_5)Sn(OH)\}_3(A\text{-}\alpha\text{-}SiW_9O_{34})]\cdot 13H_2O$ (**Cs-2**), and $Cs_8[\{(C_6H_5)Sn(OH)\}_3(A\text{-}\alpha\text{-}H_3SiW_9O_{34})_2]\cdot 23H_2O$ (**Cs-3**), respectively. We have investigated in detail the similarities and differences in the reactivity of $(C_6H_5)Sn^{3+}$ with $[A\text{-}\alpha\text{-}GeW_9O_{34}]^{10-}$ vs $[A\text{-}\alpha\text{-}SiW_9O_{34}]^{10-}$. All five compounds have been characterized in the solid state by means of elemental analysis, infrared spectroscopy, thermogravimetry, and single-crystal X-ray diffraction, representing the first structural analysis for polyanions **1**−**3**. A full solution characterization of **1** by multinuclear NMR spectroscopy (^1H, ^{13}C, ^{119}Sn, and ^{183}W) has also been performed. The monomeric polyanions **1** and **2** are closely associated in the solid state through (Sn)O−H···O_t (O_t: terminal oxygen atom) hydrogen bonds reinforced by weak C−H···O_t contacts to form 2-dimensional (**CsNa-1** and **CsNa-2**) or 1-dimensional (**Cs-H1**) arrangements, and also dimeric entities (**Cs-2**) depending on the network of intermolecular interactions.

Introduction

Polyoxometalates (POMs) are anionic metal-oxygen clusters with a multitude of interesting properties and a remarkable compositional, electronic, and structural diversity. These features endow POMs with potential applications in a wide range of fields, including catalysis, medicine, and materials science.[1]

The derivatization of POMs with organometallic moieties covalently attached to the metal-oxo framework constitutes an emerging area of interest because the resulting hybrid species combine the unique features of both components. Hence the systematic functionalization of POMs can lead to assemblies with novel structures and may allow for a rational design of tailored catalytic systems, an increase of the selectivity to specific targets, or other unexpected synergistic effects. Substituted polyanions are also interesting building blocks for crystal engineering because they can establish a variety of networks of intermolecular interactions so that their properties and applications could be influenced. Nevertheless, the structure-activity-application relation is not yet fully understood, and therefore the synthesis of new hybrid organic-inorganic polyanions (as well as the complete structural characterization of known species) remains an important research objective.

Organotin groups are good candidates for the derivatization of POMs because the size of Sn(IV) is appropriate to substitute addenda metal centers in POM skeletons and also because the Sn−C bond shows a relatively high stability to hydrolysis in aqueous media. The groups of Pope,[2] Knoth,[3] Liu,[4] and Hasenknopf[5] have demonstrated that monoorganotin moieties (RSn^{3+}) can be easily incorporated in the vacant sites of lacunary Keggin and Wells-Dawson heteropolytungstates. This work has resulted in several examples of monomeric and dimeric sandwich-type polyanions con-

* To whom correspondence should be addressed. E-mail: u.kortz@jacobs-university.de. Tel.: +49-421-200 3235. Fax: +49-421-200 3229.
† Current address: Instituto de Ciencia Molecular (ICMol), Universidad de Valencia, Polígono de la Coma s/n, E-46980 Paterna, Valencia, Spain.

10.1021/ic800852d CCC: $40.75
Published on Web 09/04/2008

taining tightly bound RSn^{3+} functionalities. These hybrid polyanions fulfill the essential requirements for pharmaceutical applications by being water-soluble and stable at physiological pH.[6] A few years ago, our group introduced the use of diorganotin units (R_2Sn^{2+}) as linkers of polyoxotungstates and -molybdates to construct large, discrete clusters with unprecedented architectures (examples including monomeric to dodecameric assemblies),[7] and also extended materials with dimensionalities ranging from 1 to 3.[8]

Earlier work by Pope and co-workers[2c] on the interaction of RSn^{3+} ($R = n\text{-}C_4H_9$, C_6H_5) electrophiles toward *A*-α- and *A*-*β*-trilacunary Keggin tungstosilicates resulted in eight such hybrid polyanions. Although these species were fully studied in solution by multinuclear NMR techniques, the solid state characterization was incomplete. Only two of the eight compounds were characterized by single-crystal X-ray diffraction, namely the trisubstituted monomeric Keggin cluster $[\{(C_6H_5)Sn(OH)\}_3(A\text{-}\beta\text{-}SiW_9O_{34})]^{4-}$ and the dimeric sandwich-type polyanion $[\{(n\text{-}C_4H_9)Sn(OH)\}_3(A\text{-}\alpha\text{-}H_3SiW_9O_{34})_2]^{8-}$. Furthermore, two other compounds lacked a complete formula because of the absence of elemental analyses.

To our knowledge, no organotin derivatives of trilacunary Keggin tungstogermanates have been reported. Therefore, we decided to carry out a study on the reactivity of RSn^{3+} electrophiles toward 9-tungstogermanates to identify the similarities and differences between both $RSn^{3+}/[XW_9O_{34}]^{10-}$ ($X = Ge^{IV}$, Si^{IV}) systems. We also decided to reinvestigate the reactivity for the 9-tungstosilicate analogues to complete the solid state characterization of these hybrid polyanions.

Here we report the synthesis, solution and solid state structures of the first trilacunary Keggin tungstogermanate functionalized with organotin units, $[\{(C_6H_5)Sn(OH)\}_3(A\text{-}\alpha\text{-}GeW_9O_{34})]^{4-}$ (**1**), and of two organotin-containing 9-tungstosilicates, $[\{(C_6H_5)Sn(OH)\}_3(A\text{-}\alpha\text{-}SiW_9O_{34})]^{4-}$ (**2**) and $[\{(C_6H_5)Sn(OH)\}_3(A\text{-}\alpha\text{-}H_3SiW_9O_{34})_2]^{8-}$ (**3**). These polyanions were isolated in the form of five different compounds by reaction of $(C_6H_5)SnCl_3$ with $Na_{10}[A\text{-}\alpha\text{-}XW_9O_{34}]\cdot 18H_2O$ ($X = Si^{IV}$, Ge^{IV}) in water: $Cs_3Na[\{(C_6H_5)Sn(OH)\}_3(A\text{-}\alpha\text{-}GeW_9O_{34})]\cdot 9H_2O$ (**CsNa-1**), $Cs_3[\{(C_6H_5)Sn(OH)\}_3(A\text{-}\alpha\text{-}HGeW_9O_{34})]\cdot 8H_2O$ (**Cs-H1**), $Cs_3Na[\{(C_6H_5)Sn(OH)\}_3(A\text{-}\alpha\text{-}SiW_9O_{34})]\cdot 9H_2O$ (**CsNa-2**), $Cs_4[\{(C_6H_5)Sn(OH)\}_3(A\text{-}\alpha\text{-}SiW_9O_{34})]\cdot 13H_2O$ (**Cs-2**), and $Cs_8[\{(C_6H_5)Sn(OH)\}_3(A\text{-}\alpha\text{-}H_3SiW_9O_{34})_2]\cdot 23H_2O$ (**Cs-3**).

Experimental Section

Materials and Methods. The precursors $Na_{10}[A\text{-}\alpha\text{-}XW_9O_{34}]\cdot 18H_2O$ ($X = Si^{IV}$, Ge^{IV}) were synthesized according to literature procedures and identified by infrared spectroscopy.[9] All other chemicals were purchased from commercial sources and used without further purification. Elemental analyses were performed by Analytische Laboratorien, Lindlar, Germany. Infrared spectra were obtained as KBr pellets on a Nicolet Avatar 370 FT-IR spectrophotometer. Thermal analyses were carried out on a TA Instruments SDT Q600 thermobalance with a 100 mL/min flow of N_2; the temperature was ramped from 20 to 800 °C at a rate of 5 °C/min. All NMR spectra were recorded at room temperature on a 400 MHz JEOL ECP400H instrument using freshly prepared reaction mixtures (pH 1−2) and D_2O as solvent; the ^{183}W NMR measurements were performed at 16.656 MHz in 10 mm tubes, and the ^{119}Sn, ^{13}C, and ^{1}H spectra were recorded in 5 mm tubes at 149.081, 100.525, and 399.782 MHz, respectively.

Synthesis of $Cs_3Na[\{(C_6H_5)Sn(OH)\}_3(A\text{-}\alpha\text{-}GeW_9O_{34})]\cdot 9H_2O$ (CsNa-1) and $Cs_3[\{(C_6H_5)Sn(OH)\}_3(A\text{-}\alpha\text{-}HGeW_9O_{34})]\cdot 8H_2O$ (Cs−H1). Powdered $Na_{10}[A\text{-}\alpha\text{-}GeW_9O_{34}]\cdot 18H_2O$ (1.35 g, 0.50 mmol) was added to a solution of $(C_6H_5)SnCl_3$ (0.30 mL, 1.79 mmol) in water (20 mL), and after stirring the reaction mixture for 30 min. at room temperature, a white precipitate was filtered off. Colorless, rhombohedral single crystals of **CsNa-1** suitable for X-ray diffraction were obtained from the filtrate by addition of a few drops of aqueous 1 M CsCl and subsequent slow evaporation at room temperature for a few days [Yield: 0.38 g (22% based on Ge)]. Polyanion **1** could also be isolated from the filtrate as a white powder of the **Cs-H1** salt by precipitation with an excess of solid CsCl (0.50 g, 2.97 mmol). Recrystallization from warm water yielded colorless, rod-like single crystals suitable for X-ray diffraction after a few weeks [Yield: 0.27 g (17% based on Ge)].

(1) (a) Pope, M. T. *Heteropoly and Isopoly Oxometalates*; Springer-Verlag: Berlin, Germany, 1983. (b) Pope, M. T.; Müller, A. *Angew. Chem., Int. Ed. Engl.* **1991**, *30*, 34. (c) *Polyoxometalates: From Platonic Solids to Antiretroviral Activity*; Pope, M. T., Müller, A., Eds.; Kluwer: Dordrecht, The Netherlands, 1994. (d) Hill, C. L., Ed.; *Chem. Rev.* **1998**, *98* (1), special thematic issue. (e) *Polyoxometalate Chemistry: From Topology via self-Assembly to Applications*; Pope, M. T., Müller, A., Eds.; Kluwer: Dordrecht, The Netherlands, 2001. (f) *Polyoxometalate Chemistry for Nanocomposite Design*; Pope, M. T., Yamase, T., Eds.; Kluwer: Dordrecht, The Netherlands, 2002. (g) *Polyoxometalate Molecular Science*; Borrás-Almenar, J. J., Coronado, E., Müller, A., Pope, M. T., Eds.; Kluwer: Dordrecht, The Netherlands, 2003. (h) Pope, M. T. In *Comprehensive Coordination Chemistry II*; McCleverty, J. A., Meyer, T. J., Eds.; Elsevier Ltd.: Oxford, U.K., 2004.

(2) (a) Zonnevijlle, F.; Pope, M. T. *J. Am. Chem. Soc.* **1979**, *101*, 2211. (b) Xin, F.; Pope, M. T. *Organometallics* **1994**, *13*, 4881. (c) Xin, F.; Pope, M. T.; Long, G. J.; Russo, U. *Inorg. Chem.* **1996**, *35*, 1207. (d) Xin, F.; Pope, M. T. *Inorg. Chem.* **1996**, *35*, 5693. (e) Sazani, G.; Dickman, M. H.; Pope, M. T. *Inorg. Chem.* **2000**, *39*, 939. (f) Sazani, G.; Pope, M. T. *Dalton Trans.* **2004**, 1989. (g) Belai, N.; Pope, M. T. *Polyhedron* **2006**, *25*, 2015.

(3) (a) Knoth, W. H. *J. Am. Chem. Soc.* **1979**, *101*, 759. (b) Knoth, W. H. *J. Am. Chem. Soc.* **1979**, *101*, 2211. (c) Knoth, W. H.; Domaille, P. J.; Roe, D. C. *Inorg. Chem.* **1983**, *22*, 818. (d) Knoth, W. H.; Domaille, P. J.; Farlee, R. D. *Organometallics* **1985**, *4*, 62.

(4) (a) Yang, Q. H.; Dai, H. C.; Liu, J. F. *Transition Met. Chem.* **1998**, *23*, 93. (b) Wang, X. H.; Dai, H. C.; Liu, J. F. *Polyhedron* **1999**, *18*, 2293. (c) Wang, X. H.; Dai, H. C.; Liu, J. F. *Transition Met. Chem.* **1999**, *24*, 600. (d) Wang, X. H.; Liu, J. F. J. *Coord. Chem.* **2000**, *51*, 73. (e) Wang, X. H.; Liu, J. T.; Zhang, R. C.; Li, B.; Liu, J. F. *Main Group Met. Chem.* **2002**, *25*, 535.

(5) (a) Bareyt, S.; Piligkos, S.; Hasenknopf, B.; Gouzerh, P.; Lacôte, E.; Thorimbert, S.; Malacria, M. *Angew. Chem., Int. Ed.* **2003**, *42*, 3404. (b) Bareyt, S.; Piligkos, S.; Hasenknopf, B.; Gouzerh, P.; Lacôte, E.; Thorimbert, S.; Malacria, M. *J. Am. Chem. Soc.* **2005**, *127*, 6788. (c) Micoine, K.; Hasenknopf, B.; Thorimbert, S.; Lacôte, E.; Malacria, M. *Org. Lett.* **2007**, *9*, 3981.

(6) Sarafianos, S. G.; Kortz, U.; Pope, M. T.; Modak, M. J. *Biochem. J.* **1996**, *319*, 619.

(7) (a) Hussain, F.; Reicke, M.; Kortz, U. *Eur. J. Inorg. Chem.* **2004**, 2733. (b) Hussain, F.; Kortz, U. *Chem. Commun.* **2005**, 1191. (c) Kortz, U.; Hussain, F.; Reicke, M. *Angew. Chem., Int. Ed.* **2005**, *44*, 3773. (d) Hussain, F.; Kortz, U.; Keita, B.; Nadjo, L.; Pope, M. T. *Inorg. Chem.* **2006**, *45*, 761. (e) Alam, M. S.; Dremov, V.; Müller, P.; Postnikov, A. V.; Mal, S. S.; Hussain, F.; Kortz, U. *Inorg. Chem.* **2006**, *45*, 2866. (f) Hussain, F.; Dickman, M. H.; Kortz, U.; Keita, B.; Nadjo, L.; Khitrov, G. A.; Marshall, A. G. *J. Cluster Sci.* **2007**, *18*, 173. (g) Keita, B.; de Oliveira, P.; Nadjo, L.; Kortz, U. *Chem.—Eur. J.* **2007**, *13*, 5480. (h) Reinoso, S.; Dickman, M. H.; Matei, M. F.; Kortz, U. *Inorg. Chem.* **2007**, *46*, 4383.

(8) (a) Reinoso, S.; Dickman, M. H.; Reicke, M.; Kortz, U. *Inorg. Chem.* **2006**, *45*, 9014. (b) Reinoso, S.; Dickman, M. H.; Kortz, U. *Inorg. Chem.* **2006**, *45*, 10422.

(9) (a) Hervé, G.; Tézé, A. *Inorg. Chem.* **1977**, *16*, 2115. (b) Tézé, A.; Hervé, G. *Inorg. Synth.* **1990**, *27*, 85.

Table 1. Crystallographic Data for Compounds **CsNa-1**, **Cs-H1**, **CsNa-2**, **Cs-2**, and **Cs-3**

	CsNa-1	Cs-H1	CsNa-2	Cs-2	Cs-3
formula	$C_{18}H_{36}Cs_3GeNaO_{46}Sn_3W_9$	$C_{18}H_{35}Cs_3GeO_{45}Sn_3W_9$	$C_{18}H_{36}Cs_3NaO_{46}SiSn_3W_9$	$C_{18}H_{44}Cs_4O_{50}SiSn_3W_9$	$C_{18}H_{70}Cs_8O_{94}Si_2Sn_3W_{18}$
fw (g mol^{-1})	3493.5	3453.5	3449.0	3631.0	6575.6
crystal system	rhombohedral	triclinic	rhombohedral	triclinic	monoclinic
space group	$R\bar{3}$	$P\bar{1}$	$R\bar{3}$	$P\bar{1}$	$C2/m$
T (K)	173(2)	173(2)	296(2)	233(2)	173(2)
a (Å)	16.8069(3)	13.5392(11)	16.75840(10)	13.6256(14)	32.8032(6)
b (Å)		14.4650(14)		15.2512(12)	16.2520(3)
c (Å)	33.8171(16)	16.5817(15)	33.6877(5)	16.7221(15)	20.9576(5)
α (deg)		69.846(3)		75.893(4)	
β (deg)		83.636(3)		76.571(5)	120.6750(10)
γ (deg)		65.343(3)		71.156(4)	
V (Å^3)	8272.6(4)	2768.6(4)	8193.45(14)	3144.6(5)	9609.5(3)
Z	6	2	6	2	4
D_{calcd} (g cm^{-3})	4.207	4.143	4.194	3.835	4.545
μ (mm^{-1})	22.621	22.520	22.322	19.959	25.346
collected reflns	33573	78476	116640	202779	78894
unique reflns (R_{int})	3666 (0.090)	7766 (0.066)	6099 (0.072)	12788 (0.124)	7540 (0.102)
obsd reflns ($I > 2\sigma(I)$)	2608	6431	4981	8919	5658
params	141	361	137	430	362
$R(F)^a$ (obsd reflns)	0.043	0.035	0.040	0.086	0.054
$wR(F^2)^a$ (all reflns)	0.096	0.100	0.125	0.137	0.167
GoF	1.065	1.019	1.016	1.052	1.078

^{a} $R(F) = \sum||F_o| - |F_c||/\sum|F_o|$; $wR(F^2) = \{\sum[w(F_o^2 - F_c^2)^2]/\sum[w(F_o^2)^2]\}^{1/2}$.

Compound CsNa-1. Anal. Calcd (found) for $C_{18}H_{36}Cs_3GeNaO_{46}Sn_3W_9$: C, 6.19 (6.27); H, 1.04 (1.21); Cs, 11.41 (10.75); Ge, 2.08 (1.83); Na, 0.66 (0.65); Sn, 10.2 (10.5); W, 47.4 (46.7). IR (cm^{-1}). 1479 (w), 1431 (w), 1077 (w), 969 (m), 893 (s), 794 (vs), 755 (sh), 697 (s), 642 (s), 525 (m), 495 (m), 451 (m), 419 (m). NMR (ppm). δ (multiplicity, relative intensity) for ^{183}W, −76.9 (s, 2, $^2J_{W-W}$ = 8 Hz), −152.5 (s, 1, $^2J_{W-W}$ = 10 Hz); ^{119}Sn, −584.3 (s, $^2J_{Sn-W}$ = 41 Hz); ^{13}C, 130.3 (s, 2), 131.5 (s, 1), 136.3 (s, 2), and 145.6 (s, 1); ^{1}H, 7.8 (m), 8.1 (q), 8.2 (m).

Compound Cs-H1. Anal. Calcd (found) for $C_{18}H_{35}Cs_3GeO_{45}Sn_3W_9$: C, 6.26 (6.36); H, 1.02 (1.15); Cs, 11.6 (12.1); Ge, 2.10 (1.68); Sn, 10.3 (10.0); W, 47.9 (47.1). IR (cm^{-1}). 1478 (w), 1431 (w), 1076 (w), 966 (m), 889 (s), 794 (vs), 759 (s), 697 (s), 640 (s), 559 (m), 525 (m), 497 (m), 451 (s), 420 (m).

Synthesis of $Cs_3Na[\{(C_6H_5)Sn(OH)\}_3(A\text{-}\alpha\text{-}SiW_9O_{34})]\cdot 9H_2O$ (CsNa-2), $Cs_4[\{(C_6H_5)Sn(OH)\}_3(A\text{-}\alpha\text{-}SiW_9O_{34})]\cdot 13H_2O$ (Cs-2), and $Cs_8[\{(C_6H_5)Sn(OH)\}_3(A\text{-}\alpha\text{-}H_3SiW_9O_{34})_2]\cdot 23H_2O$ (Cs-3). Compounds **CsNa-2** [Yield: 0.34 g (20% based on Si)] and **Cs-2** [Yield: 0.41 g (23% based on Si)] were prepared following the procedure described for the Ge analogues **CsNa-1** and **Cs-H1**, respectively, but using $Na_{10}[A\text{-}\alpha\text{-}SiW_9O_{34}]\cdot 18H_2O$ (1.36 g, 0.49 mmol). In the case of **Cs-2**, the IR spectrum of the bulk solid obtained after precipitation with solid CsCl showed, in addition to polyanion **2**, the presence of polyanion **3** as a side-product. Fractional recrystallization from warm water yielded colorless, plate-like single crystals of **Cs-3** suitable for X-ray diffraction after a few days and colorless, block-like single crystals of **Cs-2** suitable for X-ray diffraction after a few weeks.

Compound **Cs-3** was obtained in higher yield by adding solid $Na_{10}[A\text{-}\alpha\text{-}SiW_9O_{34}]\cdot 18H_2O$ (2.04 g, 0.73 mmol) to a solution of $(C_6H_5)SnCl_3$ (0.15 mL, 0.89 mmol) in water (10 mL). After stirring for 30 min at room temperature, an excess of solid CsCl (1.00 g, 5.9 mmol) was added to the resulting clear solution and a white powder was formed, which contained a mixture of **2** and **3** according to the IR spectrum. Recrystallization from warm water yielded **Cs-3** overnight as a crystalline powder [Yield: 0.29 g (15% based on Sn)].

Compound CsNa-2. Anal. Calcd (found) for $C_{18}H_{36}Cs_3NaO_{46}SiSn_3W_9$: C, 6.27 (6.15); H, 1.05 (1.19); Cs, 11.56 (10.91); Na, 0.67 (0.65); Si, 0.81 (0.80); Sn, 10.3 (10.4); W, 48.0 (47.8). IR (cm^{-1}). 1476 (w), 1429 (w), 1079 (w), 1006 (sh), 972 (m), 961 (m), 905 (vs), 891 (vs), 806 (vs), 788 (vs), 744 (s), 696 (vs), 643 (sh), 567 (m), 507 (s), 484 (sh), 447 (m). NMR (ppm). δ (multiplicity, relative intensity) for: ^{183}W, −84.2 (s, 2), −163.2 (s, 1).

Compound Cs-2. Anal. Calcd (found) for $C_{18}H_{44}Cs_4O_{50}SiSn_3W_9$: C, 5.95 (6.31); H, 1.22 (1.09); Cs, 14.6 (14.4); Si, 0.77 (0.70); Sn, 9.8 (10.3); W, 45.6 (46.1). IR (cm^{-1}). 1479 (w), 1432 (w), 1077 (w), 1004 (sh), 967 (m), 892 (vs), 805 (vs), 783 (vs), 737 (s), 701 (vs), 651 (m), 530 (m), 503 (m), 477 (m), 446 (m).

Compound Cs-3. Anal. Calcd (found) for $C_{18}H_{70}Cs_8O_{94}Si_2Sn_3W_{18}$: C, 3.29 (2.93); H, 1.07 (0.86); Cs, 16.2 (16.9); Si, 0.85 (0.80); Sn, 5.4 (5.0); W, 50.3 (49.1). IR (cm^{-1}). 1479 (w), 1430 (w), 1075 (sh), 1004 (w), 945 (m), 905 (s), 765 (vs), 702 (s), 677 (s), 527 (m), 431 (m), 404 (m). NMR (ppm). δ (multiplicity, relative intensity) for: ^{183}W, −141.8 (s, 1), −183.8 (s, 2).

X-ray Data Collection and Crystal Structure Determination. Crystallographic data for compounds **CsNa-1**, **Cs-H1**, **CsNa-2**, **Cs-2**, and **Cs-3** are summarized in Table 1. Single crystals were mounted on glass fibers (**CsNa-2**) or in Hampton cryoloops (**CsNa-1**, **Cs-H1**, **Cs-2**, and **Cs-3**) for indexing and intensity data collection at 173 K (**CsNa-1**, **Cs-H1**, and **Cs-3**), 233 K (**Cs-2**), or 296 K (**CsNa-2**), respectively. Data were collected on a Bruker X8 APEX II CCD single-crystal diffractometer with κ geometry and graphite-monochromated Mo Kα radiation (λ = 0.71073 Å). Data collections, unit cell determinations, intensity data integrations, routine corrections for Lorentz and polarization effects, and multiscan absorption corrections were performed using the APEX2 software package.[10] The structures were solved and refined using the SHELXTL software package.[11] Direct (**CsNa-1**, **CsNa-2**, **Cs-2**, and **Cs-3**) or Patterson (**Cs-H1**) methods were used to solve the structures and to locate the heavy atoms. The remaining atoms were found from successive Fourier syntheses. Heavy atoms were refined anisotropically. Hydrogen atoms of the phenyl groups were placed in calculated positions and were refined with a riding model using standard SHELXL parameters. Slightly low isotropic thermal parameters for the carbon atoms bonded to tin in **Cs-H1** suggest possible disorder with a heavier atom such as oxygen, which might result from partial hydrolysis of the tin-phenyl bond. However, the effect appears to be small, and a disorder model for these atoms

(10) *APEX2*, version 2.1−0; Bruker AXS Inc.: Madison, WI, 2005.
(11) Sheldrick, G. M. *Acta Crystallogr.* **2007**, *A64*, 112.

was not investigated. The final geometrical calculations were carried out with the PLATON program.[12]

Results and Discussion

Synthesis. To investigate the reactivity of the $(C_6H_5)Sn^{3+}$ electrophile with trilacunary 9-tungstogermanates we reacted $Na_{10}[A\text{-}\alpha\text{-}GeW_9O_{34}]\cdot 18H_2O$ with $(C_6H_5)SnCl_3$ following the conditions reported by Pope for the $(C_6H_5)Sn^{3+}/[A\text{-}\alpha\text{-}SiW_9O_{34}]^{10-}$ system.[2c] According to their results, two different hybrid tungstosilicates can be cleanly isolated as Cs salts depending on the $(C_6H_5)Sn^{3+}/[A\text{-}\alpha\text{-}SiW_9O_{34}]^{10-}$ ratio: the monomeric Keggin anion $[\{(C_6H_5)Sn(OH)\}_3(A\text{-}\alpha\text{-}SiW_9O_{34})]^{4-}$ for a 3:1 ratio; and the dimeric, sandwich anion $[\{(C_6H_5)Sn(OH)\}_3(A\text{-}\alpha\text{-}H_3SiW_9O_{34})_2]^{8-}$ for a 1:1 ratio.

Thus, reactions were carried out in water at room temperature using two $(C_6H_5)Sn^{3+}/[A\text{-}\alpha\text{-}GeW_9O_{34}]^{10-}$ ratios, 3:1 and 1:1. In both cases, the pH of the reaction mixtures was approximately 1. Isolation of the final compounds was performed following two different strategies: bulk precipitation with an excess of solid CsCl and subsequent crystallization from water, as in Pope's previous study; and direct crystallization by addition of 1 M aqueous CsCl to the final solution. Other alkali cations (Na^+, K^+, NH_4^+, and Rb^+) were also tested as crystallizing agents without satisfactory results.

Unlike for the reaction of $[A\text{-}\alpha\text{-}SiW_9O_{34}]^{10-}$ with $(C_6H_5)Sn^{3+}$, in the case of $[A\text{-}\alpha\text{-}GeW_9O_{34}]^{10-}$ a single hybrid polyanion was formed regardless of the ratio of the reactants, namely, the monomeric Keggin anion $[\{(C_6H_5)Sn(OH)\}_3(A\text{-}\alpha\text{-}GeW_9O_{34})]^{4-}$ (**1**). ^{183}W NMR solution studies performed on freshly prepared reaction mixtures of ratios 3:1 and 1:1 showed both similar, two-line spectra with chemical shifts close to those reported for the $[\{(C_6H_5)Sn(OH)\}_3(A\text{-}\alpha\text{-}SiW_9O_{34})]^{4-}$ analogue and identical intensities (relative ratios 2 to 1). We did not see any transformation of **1** to a sandwich-derivative or any other species, as the ^{183}W NMR spectra remained unchanged for several days.

Polyanion **1** could be cleanly obtained in the solid state in relatively low yield as two different salts depending on the isolation strategy: $Cs_3Na[\{(C_6H_5)Sn(OH)\}_3(A\text{-}\alpha\text{-}GeW_9O_{34})]\cdot 9H_2O$ (**CsNa-1**) by direct crystallization and $Cs_3[\{(C_6H_5)Sn(OH)\}_3(A\text{-}\alpha\text{-}HGeW_9O_{34})]\cdot 8H_2O$ (**Cs-H1**) by crystallization of the bulk precipitate. Thus, the isolation strategy has an influence on the countercation composition of the final compound but also on the degree of protonation of **1** in the solid state. The nonprotonated form of **1** is obtained from the direct crystallization strategy (**CsNa-1**), whereas the monoprotonated species is isolated when the crystallization of the bulk precipitate strategy is applied (**Cs-H1**). The nonprotonated $[\{(C_6H_5)Sn(OH)\}_3(A\text{-}\alpha\text{-}SiW_9O_{34})]^{4-}$ analogue is the species isolated by crystallization of the bulk precipitate in the case of the $(C_6H_5)Sn^{3+}/[A\text{-}\alpha\text{-}SiW_9O_{34}]^{10-}$ system.

Because no crystal structure had been reported for the phenyltin-containing tungstosilicates $[\{(C_6H_5)Sn(OH)\}_3(A\text{-}\alpha\text{-}SiW_9O_{34})]^{4-}$ (**2**) and $[\{(C_6H_5)Sn(OH)\}_3(A\text{-}\alpha\text{-}H_3SiW_9O_{34})_2]^{8-}$ (**3**), we decided to reinvestigate the reactivity for the $(C_6H_5)Sn^{3+}/[A\text{-}\alpha\text{-}SiW_9O_{34}]^{10-}$ system to complete their solid state characterization. In agreement with Pope's previous results,[2c] ^{183}W NMR spectroscopy on a freshly prepared reaction mixture with the reactants in a 3:1 ratio showed two lines assigned to **2**, indicating that this was the only species in solution. However, the IR spectrum of the bulk solid obtained after precipitation with solid CsCl revealed the presence of a minor fraction of **3** in addition to **2**. Both species were separated by fractional crystallization as $Cs_4[\{(C_6H_5)Sn(OH)\}_3(A\text{-}\alpha\text{-}SiW_9O_{34})]\cdot 13H_2O$ (**Cs-2**) and $Cs_8[\{(C_6H_5)Sn(OH)\}_3(A\text{-}\alpha\text{-}H_3SiW_9O_{34})_2]\cdot 23H_2O$ (**Cs-3**) owing to their different solubility in water, the latter crystallizing as a side-product in a few days and the former as the main product in relatively low yield in a few weeks. In contrast, the direct crystallization strategy led to the isolation of a single species, polyanion **2**, as the mixed salt $Cs_3Na[\{(C_6H_5)Sn(OH)\}_3(A\text{-}\alpha\text{-}SiW_9O_{34})]\cdot 9H_2O$ (**CsNa-2**).

According to Pope's previous study,[2c] polyanion **3** is the only product formed when the reactants are mixed in a 1:1 ratio. However, in our case four lines with relative intensities 2:1:1:2 were observed by ^{183}W NMR performed on a freshly prepared reaction mixture. These lines could be assigned to a mixture of **2** and **3** in a 2:1 ratio. After a few days, an increase of the signals of **3** was observed, together with new lines originating from other unidentified species. The IR spectrum of the solid obtained after bulk precipitation confirmed a mixture of **2** and **3**, which were separated by fractional crystallization as **Cs-2** and **Cs-3** in similar yields. Moreover, **2** was the only species isolated by direct crystallization. As in the case of the 3:1 reaction, the mixed **CsNa-2** salt was obtained in good yield.

These observations indicate that both **2** and **3** are formed when $[A\text{-}\alpha\text{-}SiW_9O_{34}]^{10-}$ is reacted with $(C_6H_5)Sn^{3+}$. In agreement with Pope's study both species are in equilibrium, which is shifted toward **2** by increasing the phenyltin:tungstosilicate ratio. We have shown that **2** can be selectively crystallized from mixtures of **2** and **3** as a mixed Cs−Na salt, probably because of a more favorable crystal packing.

Structure of Polyanions 1 and 2. Polyanions **1** and **2** are composed of a trilacunary $[A\text{-}\alpha\text{-}XW_9O_{34}]^{10-}$ ($X = Si^{IV}$, Ge^{IV}) Keggin subunit and three $(C_6H_5)Sn^{3+}$ moieties. The parent $[\alpha\text{-}XW_{12}O_{40}]^{4-}$ Keggin anion consists of a central XO_4 tetrahedral hetero group and four $\{W_3O_{13}\}$ triads (composed of three edge-sharing WO_6 octahedra) linked via corner-sharing resulting in a polyanion with ideal T_d symmetry. The *A*-type trilacunary derivative is obtained from the parent cluster by removal of three corner-sharing WO_6 octahedra. The X-ray structures of the Na and K salts of $[A\text{-}\alpha\text{-}SiW_9O_{34}]^{10-}$ have been reported,[13] but to our knowledge, no structural characterization of $[A\text{-}\alpha\text{-}GeW_9O_{34}]^{10-}$ can be found in the literature.

In **1** and **2** the vacant positions of the $[A\text{-}\alpha\text{-}XW_9O_{34}]^{10-}$ subunits are filled by three $(C_6H_5)Sn^{3+}$ groups, such that the Sn(IV) centers act as addenda atoms regenerating a hybrid, monomeric Keggin anion (see Figure 1). In the solid state

(12) Spek, A. L. *PLATON*; Utrecht Universiteit: Utrecht, The Netherlands, 2005.

(13) (a) Hubert, W.; Hartl, H. *Z. Naturforsch.* **1996**, *B51*, 969. (b) Laronze, N.; Marrot, J.; Hervé, G. *Inorg. Chem.* **2003**, *42*, 5857.

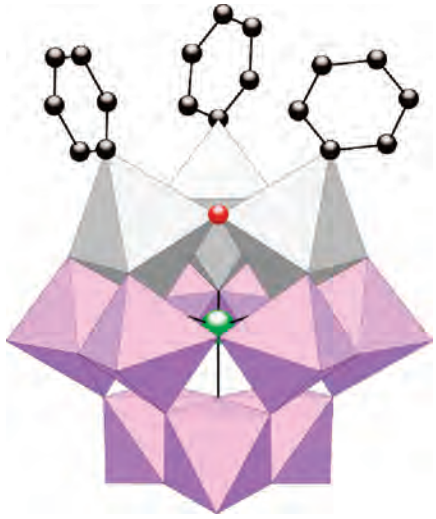

Figure 1. Combined polyhedral/ball-and-stick representation of polyanions **1** and **2**. Color code: WO_6 octahedra, lilac; $(C_6H_5)SnO_5$ octahedra, light gray; C, black; O, red; X = Ge (**1**), Si (**2**), green.

the ideal C_{3v} symmetry of the polyanions is lowered to C_3 in **CsNa-1** and **CsNa-2**, and to C_1 in **Cs-H1** and **Cs-2** because of the orientation of the phenyl rings. As previously pointed out by Pope,[2b] the W−O(Sn) bonds are in general shorter than the W−O(W) bonds (see Table 2). This fact reflects a well-known distortion phenomenon[14] that consists of alternating, *trans*-related long and short bond sequences that propagate through the POM framework, starting from the corner-shared $\{(C_6H_5)_3Sn_3O_{12}\}$ triad and ending at the opposite, edge-shared $\{W_3O_{13}\}$ triad.

According to elemental and thermal analyses, **1** is triprotonated in **CsNa-1** and tetraprotonated in **Cs-H1**, whereas **2** is triprotonated in both **CsNa-2** and **Cs-2**. Bond valence sum (BVS) calculations[15] clearly show that the three bridging O atoms between corner-sharing $(C_6H_5)SnO_5$ octahedra are protonated in all cases. This phenomenon was also observed by Pope for the hybrid Wells-Dawson anion $[\{(C_6H_5)Sn(OH)\}_3(\alpha\text{-}HP_2W_{18}O_{56})]^{5-}$.[2b] The fourth protonation site of **1** in **Cs-H1** could not be determined unambiguously, but the relatively low BVS values (1.57−1.89) of the O atoms that link Sn and W centers indicate that the fourth proton might be randomly disordered over the Sn−O_e−W bridges.

Solution NMR Characterization of Polyanion 1. The ^{119}Sn NMR spectrum displays a single resonance at δ −584.3 ppm, while the ^{183}W NMR spectrum shows two lines at δ −76.9 and δ −152.5 ppm with relative intensities 2:1 (see Figure 2). The ^{1}H- and ^{13}C NMR spectra are typical for phenyl groups with three multiplets between 7.8 and 8.2 ppm and four singlets of relative intensities 2:1:2:1 at δ 130.3, 131.5, 136.3 and 145.6 ppm, respectively (see Figure S1 in the Supporting Information). All spectra are fully consistent with the structure of **1**, assuming free rotation of the phenyl groups in solution. Our results confirm the ideal C_{3v} symmetry of **1** with three equivalent $(C_6H_5)Sn^{3+}$ moieties, six equivalent W atoms in the Keggin belt, and three equivalent W atoms in the cap.

The ^{119}Sn chemical shift of **1** is comparable to the value of δ −578 ppm reported by Pope for the tungstosilicate analogue **2**.[2c] The ^{119}Sn NMR spectrum of **1** also shows the expected satellites indicating ^{119}Sn−O−^{183}W coupling ($^2J_{Sn-W}$ = 41 Hz).[7a] In addition, the pattern observed in the ^{183}W NMR spectrum of **1** is in agreement with those pointed out by Pope for the monomeric, Keggin $[\{(RSn(OH)\}_3(A\text{-}SiW_9O_{34})]^{4-}$ tungstosilicates, that is, two lines with intensity ratio of 2:1 corresponding to the belt- and cap-tungsten atoms, respectively, where $\delta_{cap} < \delta_{belt}$.[2c] Moreover, the ^{183}W chemical shifts of **1** compare well with those of **2** (δ −85 and −166 ppm), also resulting in similar Δ parameters (76 ppm for **1** and 81 ppm for **2**, where $\Delta = |\delta_{belt} - \delta_{cap}|$). The ^{183}W NMR spectrum of **1** shows the expected satellites indicating coupling of adjacent ^{183}W nuclei ($^2J_{W-W} \sim 10$ Hz).[16] The ^{183}W NMR spectrum remains unchanged for several days, indicating that **1** doest not undergo structural modifications in solution.

Structure of Polyanion 3. Polyanion **3** is composed of two trilacunary $[A\text{-}\alpha\text{-}SiW_9O_{34}]^{10-}$ Keggin subunits linked by a belt of three $(C_6H_5)Sn^{3+}$ moieties into a sandwich-type dimer of ideal D_{3h} symmetry (see Figure 3). This ideal symmetry is lowered to C_s in the crystal packing of **Cs-3**, where **3** lies on a mirror plane containing both Si atoms and the Sn1 center. The trilacunary subunits exhibit an eclipsed configuration and the W−O bond lengths are comparable to those found in **1** and **2**, with W−O(Sn) bonds (1.816(15)−1.907(16) Å) shorter than the W−O(W) bonds (1.828(15)−2.039(15) Å) as a result of the distortion phenomenon mentioned above. The Sn atoms show distorted octahedral $(C_6H_5)SnO_5$ geometries with the terminal O atoms of two edge-shared $\{W_2O_{10}\}$ dimers in the equatorial plane and the axial phenyl groups arranged in a nearly orthogonal fashion. The internal axial positions of Sn are occupied by oxo ligands, which are monoprotonated as indicated by BVS calculations. The Sn−O bond lengths are all regular (2.03(3)−2.093(15) Å), whereas the Sn−C bond lengths are 2.11(3) Å for Sn1 and 2.225(12) Å for Sn2. This type of assembly is similar to that observed for the *n*-butyltin analogue[2c] and for the phenyltin-containing tungstophosphate $K_{11}H[\{(C_6H_5)Sn(OH)\}_3(A\text{-}\beta\text{-}PW_9O_{34})_2]$, but in the latter the three aromatic rings are coplanar and one of the internal axial ligands is assumed to be a water molecule.[2b] According to elemental and thermal analyses, polyanion **3** is nonaprotonated in **Cs-3**, but BVS calculations could only locate the three protons on the internal oxo ligands, with the remaining six protons being probably disordered over the (Sn)W−O−W bridges of both Keggin subunits.

Infrared Spectroscopy. The presence of the $(C_6H_5)Sn^{3+}$ moiety can be established by three single peaks of weak intensity above 1000 cm^{-1} (see Figure S2 in the Supporting Information). Two of them are observed at approximately 1480 and 1430 cm^{-1} and are assigned to the stretching

(14) (a) Reinoso, S.; Vitoria, P.; San Felices, L.; Lezama, L.; Gutiérrez-Zorrilla, J. M. *Chem.—Eur. J.* **2005**, *11*, 1538. (b) Garvey, J. F.; Pope, M. T. *Inorg. Chem.* **1978**, *17*, 1115.

(15) Brown, I. D.; Altermatt, D. *Acta Crystallogr.* **1985**, *B41*, 244.

(16) (a) Sveshnikov, N. N.; Pope, M. T. *Inorg. Chem.* **2000**, *39*, 591. (b) Lefebvre, J.; Chauveau, F.; Doppelt, P. *J. Am. Chem. Soc.* **1981**, *103*, 4589.

Table 2. Ranges of Bond Lengths [Å] for Polyanions **1** and **2** in the Compounds **CsNa-1**, **Cs-H1**, **CsNa-2**, and **Cs-2**

	1		**2**	
	CsNa-1	**Cs-H1**	**CsNa-2**	**Cs-2**
W−O_v(W)[a]	1.865(9)−1.954(7)	1.871(8)−1.959(8)	1.854(6)−1.949(6)	1.848(10)−1.980(13)
W−O_e(W)[a]	1.910(8)−1.956(9)	1.917(9)−1.967(9)	1.904(10)−1.956(6)	1.904(9)−1.964(9)
W−O_e(Sn)[a]	1.842(7), 1.889(7)	1.843(9)−1.938(10)	1.832(6), 1.860(6)	1.823(13)−1.851(12)
W−O_t[a]	1.705(6)−1.723(8)	1.702(9)−1.731(8)	1.699(8)−1.724(9)	1.698(11)−1.760(9)
W−O_c[a]	2.312(7)−2.421(7)	2.316(7)−2.406(7)	2.382(6)−2.476(6)	2.386(9)−2.460(9)
Sn−O_v(Sn)[a]	2.090(7), 2.092(10)	2.055(8)−2.097(10)	2.076(7), 2.086(6)	2.047(9)−2.090(10)
Sn−O_e(W)[a]	2.050(7), 2.059(9)	2.057(6)−2.074(8)	2.050(6), 2.051(7)	2.050(11)−2.085(9)
Sn−C	2.128(11)	2.125(8)−2.141(8)	2.142(7)	2.109(19)−2.156(19)
Sn−O_c[a]	2.211(7)	2.234(8)−2.240(10)	2.255(6)	2.230(13)−2.299(12)
X-O_c[a,b]	1.758(10), 1.761(14)	1.739(7)−1.753(7)	1.630(11), 1.640(5)	1.619(13)−1.651(8)

[a] O_v, bridging oxygen atoms between corner-sharing octahedra; O_e, bridging oxygen atoms between edge-sharing octahedra; O_t, terminal oxygen atoms; O_c, oxygen atoms of the central XO_4 tetrahedron. [b] X = Ge^{IV} (**1**), Si^{IV} (**2**).

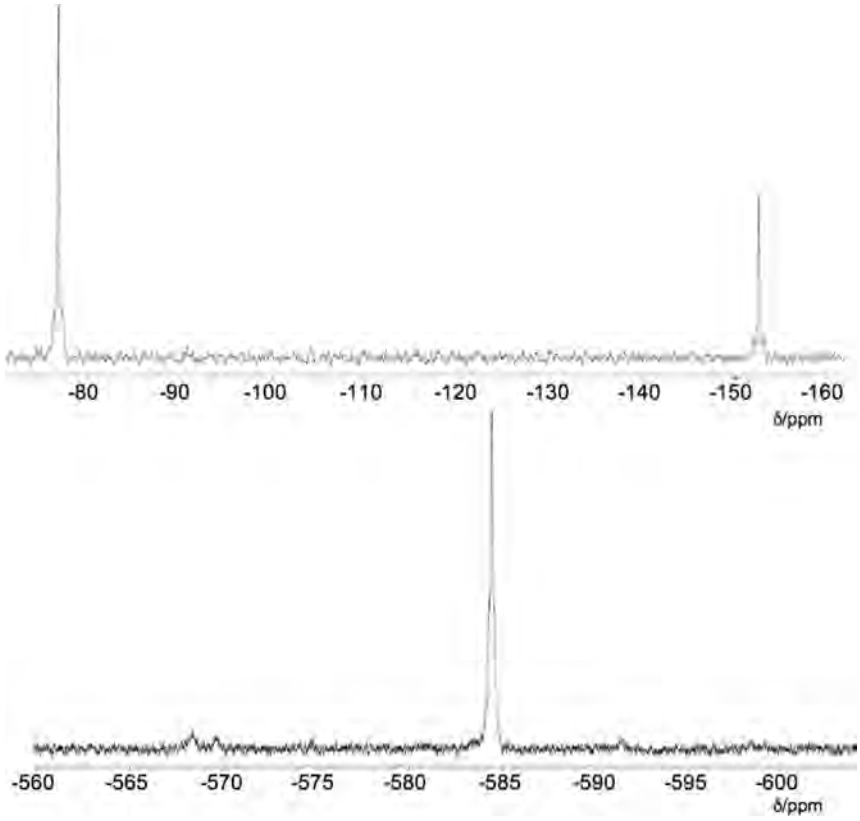

Figure 2. Solution ^{183}W NMR (top) and ^{119}Sn NMR (bottom) spectra for polyanion **1** recorded on freshly prepared reaction mixtures.

vibrations of the C−C double bonds.[17] More specifically, the peak at 1480 cm^{-1} is attributed to the C_{ipso}−C_{ortho} and C_{meta}−C_{para} bonds, whereas the peak at 1430 cm^{-1} originates from the C_{ortho}−C_{meta} bonds. A third peak appears in the range 1075−1080 cm^{-1}, and it is characteristic for the *q* vibration mode of $(C_6H_5)M^{n+}$ groups.[18]

The bands below 1000 cm^{-1} are attributed to the metal-oxo polyanion bonds. Comparing the IR spectra of the [*A*-α-$XW_9O_{34}]^{4-}$ (X = Si^{IV}, Ge^{IV}) precursors with those of **1**, **2**, and **3** reveals some similarities in the overall shape of the spectra but also significant changes in several band positions and intensities. This indicates functionalization of the precursors with retention of the trilacunary Keggin framework in the products.

Polyanions **1** and **2** show similar spectra with medium to strong peaks in the ranges 960−970 and 890−900 cm^{-1}, associated with the antisymmetric stretching vibrations of the X−O and the W−O_t bonds [ν_{as}(W−O_t) and ν_{as}(W−O_t) + ν_{as}(X−O), respectively]; strong to very strong bands at approximately 800 and 695 cm^{-1} originate from the antisymmetric stretching of the (Sn)W−O−W(Sn) bridges; and medium intensity peaks below 560 cm^{-1} correspond to bending vibrations of the central XO_4 group and the (Sn)W−O−W(Sn) bridges. In the case of **2**, splitting of the bands above 800 cm^{-1} is observed, especially for **CsNa-2**, as well as an extra shoulder at 1006 cm^{-1} assigned to a ν_{as}(W−O_t) + ν_{as}(X−O) combination. These spectra are reminiscent of those of the plenary $[XW_{12}O_{40}]^{4-}$ Keggin anions, indicating incorporation of three RSn^{3+} groups into the vacant sites of the trilacunary precursor to yield a monomeric Keggin polyanion. The bands are in general blueshifted as a result of the decrease of the ideal symmetry from T_d to C_{3v}, and they

(17) Pretsch, E.; Clerc, T.; Seibl, J.; Simon, W. *Tabellen zur Strukturaufklärung Organischer Verbindungen mit Spektroskopischen Metoden*; Springer Verlag: Berlin, Germany, 1976.
(18) Nakamoto, K. *Infrared and Raman Spectra of Inorganic and Coordination Compounds*; Wiley Interscience: New York, 1997.

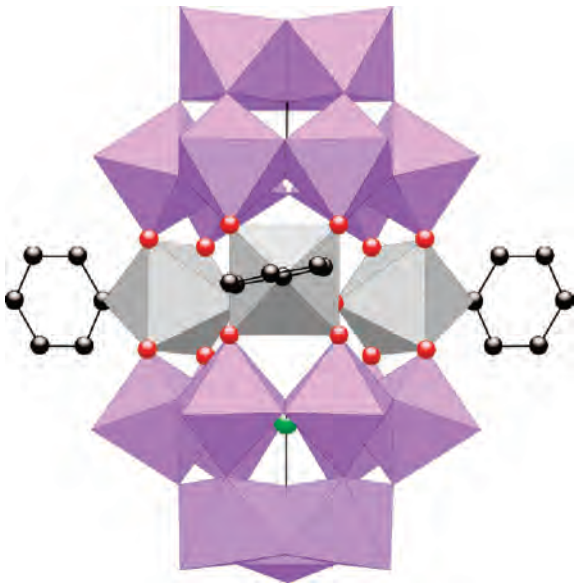

Figure 3. Combined polyhedral/ball-and-stick representation of polyanion **3**. Color code: same as Figure 1.

appear at wavenumbers in between those of the plenary and the trilacunary species, a fact characteristic of transition metal substituted Keggin polyanions.[19]

IR spectroscopy also allows to clearly distinguish the sandwich polyanion **3** from the monomeric **2** despite being composed of identical building blocks. The main differences are encountered in the bands originating from the ν_{as}(M−O_b−M) vibration modes. The ν_{as}(W−O_t) band of **3** (945 cm^{-1}) is blueshifted with respect to that of **2** (967 cm^{-1}), and the ν_{as}(M−O_b−M) bands of **3** (765, 702, and 677 cm^{-1}) are blueshifted compared to the trilacunary precursor (865, 808, and 712 cm^{-1}).

Thermal Analysis. Thermal analysis shows similar trends for **CsNa-1**, **Cs-H1**, **CsNa-2**, and **Cs-2** (see Figures S6 and S7 in the Supporting Information). Decomposition starts at room temperature with an endothermic dehydration step around 155−175 °C (**CsNa-1**, 165; **Cs-H1**, 175; **CsNa-2**, 165; **Cs-2**, 155 °C). This step involves the release of 9 water molecules for **CsNa-1** and **CsNa-2** [% calcd (found): **CsNa-1**, 4.64 (4.75); **CsNa-2**, 4.70 (4.70)], and 8 for **Cs-H1** [% calcd (found): 4.17 (4.47)]. Samples of **Cs-2** lost crystallinity upon contact with air, so that only 10 of the 13 hydration water molecules observed by X-ray crystallography could be determined [% calcd (found): 5.04 (4.88)].

Immediately after dehydration, these compounds undergo loss of the phenyl groups indicated by an exothermic mass loss step around 480 °C [% calcd for C_6H_5 (found): **CsNa-1**, 5.25 (5.43); **Cs-H1**, 5.31 (5.65); **CsNa-2**, 5.31 (5.45); **Cs-2**, 5.12 (5.91)]. After a narrow thermal stability range of the resulting polyanion (**CsNa-1**, 480−530; **Cs-H1**, −520; **CsNa-2**, −540; **Cs-2**, −520 °C), decomposition of the metal-oxo framework takes place in a third step comprising several, highly overlapping exothermic steps. This process ends at temperatures of around 700 °C (**CsNa-1**, 725; **Cs-H1**, 680; **CsNa-2**, 680; **Cs-2**, 690 °C) leading to thermally stable final residues [% calcd (found): **CsNa-1**, 88.6 (87.9) for $Cs_3GeNaO_{37}Sn_3W_9$; **Cs-H1**, 88.8 (88.3) for $Cs_3GeO_{36.5}Sn_3W_9$; **CsNa-2**, 88.5 (87.9) for $Cs_3NaO_{37}SiSn_3W_9$; and **Cs-2**, 88.4 (87.5) for $Cs_4O_{37}SiSn_3W_9$].

In the case of **Cs-3**, decomposition starts with an endothermic dehydration step involving the release of 23 water molecules [% calcd (found): 6.30 (6.22)]. Dehydration takes place up to 285 °C (see Figure S8 in the Supporting Information), and it is immediately followed by loss of the phenyl groups and decomposition of the metal-oxo framework in a single mass loss step comprising several, highly overlapping exothermic processes. The thermally stable final residue is formed above 730 °C [% calcd (found): 89.3 (90.6) for $Cs_8O_{68}Si_2Sn_3W_{18}$].

Description of the Crystal Packings. Polyanions **1** and **2** closely associate in the solid state through a variety of networks of intermolecular interactions, resulting in distinct differences in the crystal packing of compounds **CsNa-1**, **CsNa-2**, **Cs-H1**, and **Cs-2**.

Each polyanion in the isostructural compounds **CsNa-1** and **CsNa-2** is connected to three neighboring clusters through (Sn)O−H···O hydrogen bonds involving the three protonated bridging O atoms between corner-sharing $(C_6H_5)SnO_5$ octahedra and the terminal O2T atoms [see Figure 4 (a)]. This type of POM association is reinforced by weak C6−H6···O contacts with the terminal O1T atoms, resulting in a 2-dimensional arrangement of polyanions parallel to the *ab* plane. These corrugated layers display nearly circular intralamellar spaces where the Cs and $[\{(H_2O)_3Na\}_2(\mu\text{-}H_2O)_3]^{2+}$ cations and the hydration water molecules are located (see Figure S11 in the Supporting Information). The layers pack along the [001] direction with the phenyl rings pointing to the interlamellar space, so that each phenyl ring is involved in C−H···π interactions with two aromatic rings from an adjacent cluster resulting in a tilted, nearly perpendicular *off-set* arrangement (see Figure S12 in the Supporting Information).

In the case of **Cs-H1**, the (Sn)O−H···O hydrogen bonding is established by two of the three protonated bridging O atoms (O12S and O13S) and the terminal O8T and O9T atoms, whereas the third one is hydrogen bonded to a hydration water molecule. Thus, each polyanion is connected to two neighboring clusters, forming *zig-zag* chains parallel to the crystallographic *a* axis instead of the layers observed for **CsNa-1** and **CsNa-2** [see Figure 4 (b)]. This 1-dimensional POM arrangement is further stabilized by weak C−H···O contacts involving the terminal O2T and O3T atoms and the phenyl ring C1−C6, which is embedded in between the polyanions. The hybrid chains are accompanied by the Cs cations in layers parallel to the *ac* plane, which pack with the C7−C12 and C13−C18 rings occupying the interlamellar space in such a way that a sequence of hydrophilic and hydrophobic regions is formed along the [010] direction (see Figure S13 in the Supporting Information). Interlamellar, hydrophobic C−H···π interactions are established between the C13−C18 ring and the C1−C6 and C7−C12 rings.

(19) San Felices, L.; Vitoria, P.; Gutiérrez-Zorrilla, J. M.; Lezama, L.; Reinoso, S. *Inorg. Chem.* **2006**, *45*, 7748.

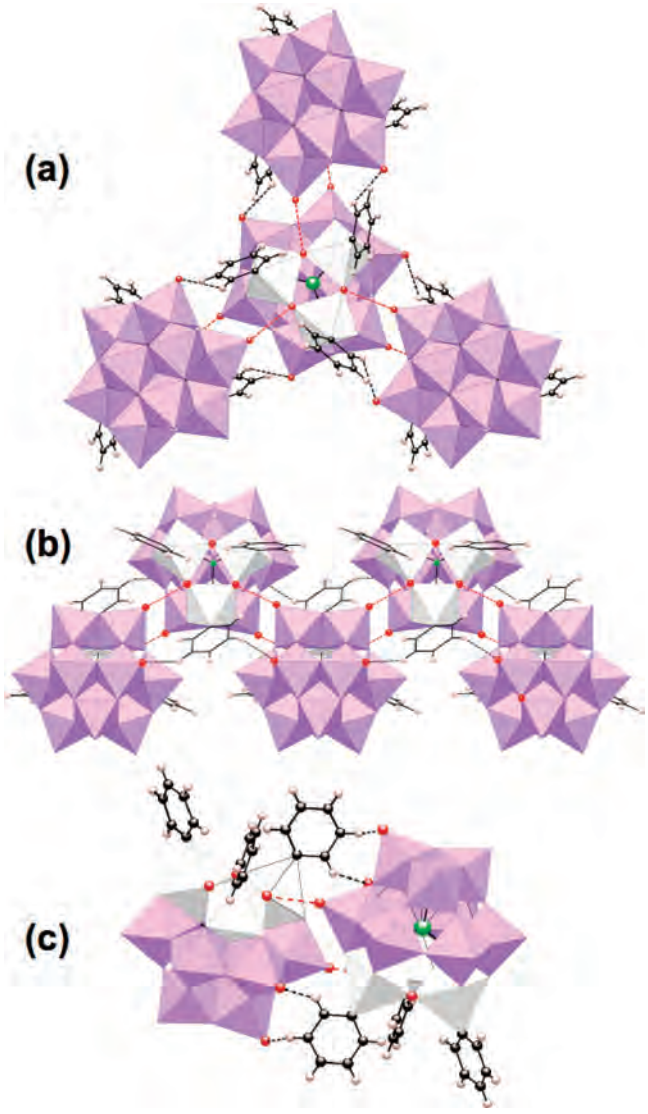

Figure 4. Networks of intermolecular (Sn)O−H···O_t (dashed red lines) and C−H···O_t (dashed black lines) interactions between polyanions **1** or **2**. (a) 2-Dimensional lattice in the crystal packing of **CsNa-1** and **CsNa-2**. (b) 1-Dimensional lattice in the crystal packing of **Cs-H1**. (c) Dimeric entity in the crystal packing of **Cs-2**. Color code: same as Figure 1. Hydrogen atoms are shown as small pink balls.

On the other hand, two of the three protonated bridging O atoms are hydrogen bonded to hydration water molecules in compound **Cs-2**. Therefore, each polyanion is connected to only one neighboring cluster through (Sn)O12S−H···O9T hydrogen bonds, forming dimers further stabilized by C−H···O interactions involving the phenyl ring C1−C6 and the terminal O3T and O4T atoms (see Figure 4c). These dimeric entities are linked by the Cs cations in layers parallel to the (011) plane, where the C7−C12 intralamellar rings are arranged nearly perpendicular to the plane of the layer and pointing to the center of the W2−W7−W8 triads of adjacent dimers (see Figure S14 in the Supporting Information). The layers pack along the [011] direction with the C1−C6 and C13−C18 rings occupying the interlamellar space, so that a sequence of hydrophilic and hydrophobic regions is formed along this direction with a scheme of interlamellar C−H···π interactions analogous to that observed for compound **Cs-H1**.

Conclusions

Our work has demonstrated that, unlike the $(C_6H_5)Sn^{3+}$/$[A\text{-}\alpha\text{-}SiW_9O_{34}]^{10-}$ system,[2c] the reaction of $(C_6H_5)SnCl_3$ with $Na_{10}[A\text{-}\alpha\text{-}GeW_9O_{34}]$ in water results in the formation of a single species, $[\{(C_6H_5)Sn(OH)\}_3(A\text{-}\alpha\text{-}GeW_9O_{34})]^{4-}$ (**1**), regardless of the ratio of reactants employed. This work nicely illustrates how a slight modification of a lacunary POM precursor, and more specifically the size of the heteroatom, entirely modifies its reactivity. Polyanion **1** represents the first organotin derivative of a trilacunary Keggin tungstogermanate and it comprises a plenary Keggin structure of ideal C_{3v} symmetry where a corner-shared $\{W_3O_{15}\}$ triad is substituted by a $\{(C_6H_5)_3Sn_3O_{12}\}$ group of three corner-sharing $(C_6H_5)SnO_5$ octahedra with protonated Sn−O−Sn bridges. Polyanion **1** is stable in solution as shown by the expected 2-line pattern (2:1) in the ^{183}W NMR spectrum, together with the 1- and 4-line patterns in the ^{119}Sn- and ^{13}C NMR spectra. On the other hand, the crystal structures of the known phenyltin-containing tungstosilicates $[\{(C_6H_5)Sn(OH)\}_3(A\text{-}\alpha\text{-}SiW_9O_{34})]^{4-}$ (**2**) and $[\{(C_6H_5)Sn(OH)\}_3(A\text{-}\alpha\text{-}H_3SiW_9O_{34})_2]^{8-}$ (**3**) are also reported. Polyanion **2** is the silicon analogue of **1**, whereas polyanion **3** displays a sandwich-type dimer with ideal D_{3h} symmetry, being composed of two $[A\text{-}\alpha\text{-}SiW_9O_{34}]^{10-}$ subunits linked by a belt of three $(C_6H_5)Sn^{3+}$ moieties. Both polyanions **1** and **2** can be prepared as different Cs salts depending on the isolation strategy: $Cs_3Na[\{(C_6H_5)Sn(OH)\}_3(A\text{-}\alpha\text{-}GeW_9O_{34})]\cdot 9H_2O$ (**CsNa-1**) or $Cs_3[\{(C_6H_5)Sn(OH)\}_3(A\text{-}\alpha\text{-}HGeW_9O_{34})]\cdot 8H_2O$ (**Cs-H1**), and $Cs_3Na[\{(C_6H_5)Sn(OH)\}_3(A\text{-}\alpha\text{-}SiW_9O_{34})]\cdot 9H_2O$ (**CsNa-2**) or $Cs_4[\{(C_6H_5)Sn(OH)\}_3(A\text{-}\alpha\text{-}SiW_9O_{34})]\cdot 13H_2O$ (**Cs-2**). The mixed salts **CsNa-1** and **CsNa-2** are obtained when a direct crystallization procedure is applied, whereas the salts **Cs-H1** and **Cs-2** are the result of crystallizing a bulk precipitate. The direct crystallization procedure allows to selectively crystallize **2** from mixtures of **2** and **3**. Polyanions **1** and **2** constitute interesting building blocks in the field of crystal engineering because they can lead to different patterns of intermolecular interactions. These clusters are closely associated in the solid state through (Sn)O−H···O_t hydrogen bonds reinforced by weak C−H···O_t contacts to form 2-dimensional (**CsNa-1** and **CsNa-2**) or 1-dimensional extended lattices (**Cs-H1**), and also dimeric entities (**Cs-2**), displaying in all cases an additional network of hydrophobic C−H···π contacts that can be regarded as a model for the association of these species in solution. Currently, we are carrying out analogous investigations on the reactivity of the $(C_6H_5)Sn^{3+}$ electrophile toward the $[A\text{-}\beta\text{-}XW_9O_{34}]^{10-}$ (X = Si^{IV}, Ge^{IV}) POM precursors.

Acknowledgment. U.K. thanks Jacobs University and the Fonds der Chemischen Industrie for research support. S.R. thanks Pablo Vitoria (Universidad del País Vasco) for scientific discussions and Gobierno Vasco/Eusko Jaurlaritza for his postdoctoral fellowship.

Supporting Information Available: Solution ^{13}C, and ^{1}H NMR spectra for polyanion **1** recorded on freshly prepared reaction mixtures. Fourier transform infrared spectra and thermogravimetric analysis/differential scanning calorimetry curves for compounds **CsNa-1**, **Cs-H1**, **CsNa-2**, **Cs-2**, and **Cs-3**. ORTEP views for polyanions **1**, **2** and **3**. Figures of the crystal packing of compounds **CsNa-1**, **CsNa-2**, **Cs-H1**, and **Cs-2**. X-ray crystallographic files of compounds **CsNa-1**, **Cs-H1**, **CsNa-2**, **Cs-2**, and **Cs-3** in CIF format. This material is available free of charge via the Internet at http://pubs.acs.org.

IC800852D